

受人
82-10-146
高工

DEUTSCHES ELEKTRONEN-SYNCHROTRON DESY

DESY 82-060
September 1982

Differential 3-Jet cross section in e^+e^- -Annihilation and Comparison
with 2nd-order predictions of QCD and Abelian Vector Theory

JADE Collaboration

NOTKESTRASSE 85 · 2 HAMBURG 52

DESY behält sich alle Rechte für den Fall der Schutzrechtserteilung und für die wirtschaftliche Verwertung der in diesem Bericht enthaltenen Informationen vor.

DESY reserves all rights for commercial use of information included in this report, especially in case of filing application for or grant of patents.

**To be sure that your preprints are promptly included in the
HIGH ENERGY PHYSICS INDEX ,
send them to the following address (if possible by air mail) :**

**DESY
Bibliothek
Notkestrasse 85
2 Hamburg 52
Germany**

Differential 3-Jet Cross Section in e^+e^- -Annihilation and Comparison
with 2nd-order Predictions of QCD and Abelian Vector Theory

JADE Collaboration

W. Bartel, D. Cords, G. Dietrich, P. Dittmann¹, R. Eichler², R. Felst, D. Haidt,
H. Krehbiel, K. Meier, B. Naroska, L.H. O'Neill³, P. Steffen
Deutsches Elektronen-Synchrotron DESY, Hamburg, Germany

E. Elsen, A. Petersen, P. Warming, G. Weber

II. Institut für Experimentalphysik

G. Kramer, G. Schierholz

II. Institut für Theoretische Physik

Universität Hamburg, Germany

S. Bethke, J. Heintze, G. Heinzelmann, K.H. Hellensbrand,

R.D. Heuer, J. von Krogh, P. Lennert, S. Kawabata⁴, S. Komamiya, H. Matsumura,

T. Nozaki, J. Olsson, H. Rieseberg, A. Wagner

Physikalisches Institut der Universität Heidelberg, Germany

A. Bell, F. Foster, G. Hughes, H. Wriedt

University of Lancaster, England

J. Allison, A.H. Ball, G. Bamford, R. Barlow, C. Bowdery, I.P. Duerdath,

I. Glendinning, F.K. Loebinger, A.A. Macbeth, H. McCann, H.E. Mills,

P.G. Murphy, P. Rowe, K. Stephens

University of Manchester, England

D. Clarke, M.C. Goddard, R. Marshall, G.F. Pearce

Rutherford Appleton Laboratory, Chilton, England

J. Kanzaki, T. Kobayashi, M. Koshihara, M. Minowa, M. Nozaki, S. Odaka,

S. Orito, A. Sato, H. Takeda, Y. Totsuka, Y. Watanabe⁵, S. Yamada,

C. Yanagisawa⁵

Lab. of Int. Coll. on Elementary Particle Physics and Department of Physics,

University of Tokyo, Japan

¹ deceased

² now at Labor f. Hochenergiephysik der ETH-Zürich, Villigen, Switzerland

³ now at Bell Laboratories, Whippany, N.Y., U.S.A.

⁴ now at KEK, Oho-machi, Tsukuba-Gun, Ibaraki-Ken, Japan

⁵ now at Rutherford Appleton Laboratory, Chilton, England

Abstract:

Differential 3-jet cross sections have been measured in e^+e^- -annihilation at an average c.m. energy of 33.8 GeV and were compared to 1st and 2nd-order predictions of QCD and of a QED-like Abelian vector theory. QCD provides a good description of the observed distributions. The inclusion of 2nd-order effects reduced the observed quark coupling strength by about 20% to $\alpha_s = 0.16 \pm 0.015$ (stat.) ± 0.03 (system.). The Abelian vector theory is found to be incompatible with the data.

High energy e^+e^- -annihilation into hadrons provides unique possibilities to test QCD. For example, the total cross section is explained by perturbative QCD, and detailed tests have been performed by several groups ¹⁾.

Remarkable qualitative agreement between the order α_s predictions ²⁾ and the data has been found. In addition ³⁾, there is strong evidence for the gluon to have spin 1, and, more recently first experimental evidence ⁴⁾ of 4-jet structure, as predicted by higher-order QCD diagrams ⁵⁾, has been reported.

In this letter we present an analysis of 3-jet events and compare the resulting differential cross sections with theoretical predictions which include all second order diagrams. Since QCD reveals its full gauge structure only in second order, it is of considerable interest to test whether the 2nd-order predictions are sensitive to its non-Abelian nature giving rise to the gluon self-coupling.

In order to elucidate this point we compare the data not only with QCD but also with an Abelian vector theory. The comparison uses the second order QCD results of ref. 6), which are based on jet definitions closely related to observable quantities. For a recent discussion of these results in comparison with other second order QCD calculations see ref.7. The cross sections for the Abelian vector theory are obtained from the expressions of ref. 6) by replacing the group constants of SU(3) by the ones of U(1).

The analysis is based on data measured with the JADE detector at center of mass energies \sqrt{s} of the e^+e^- storage ring PETRA between 30 GeV and 36.7 GeV with a luminosity weighted average of $\sqrt{s} = 33.8$ GeV. A detailed description of the detector, the trigger conditions and the criteria for the selection of hadronic events is given in ref. 8). In addition to the cuts mentioned there, events with a missing momentum exceeding half the beam energy were rejected and an acceptance cut was imposed on the angle θ between the event sphericity axis and the beam direction $|\cos\theta| < 0.83$.

The 4799 events remaining after these cuts were subjected to a jet search algorithm allowing for an arbitrary number of jets. Each event was then categorised according to the number of jets found. This event classification depends on the definition of a particle jet. In order to estimate to what extent the final results depend on the jet definition used, we pursue two different methods, which both aim for a particle jet definition similar to the definitions used in ref. 6) for the partons. The first method is the angular cluster algorithm described in detail in ref. 9) which proceeds via the following steps: 1) particles (charged or neutral) within 30° of each other are combined to form preclusters, single isolated particles are also regarded as preclusters; 2) preclusters within an angle χ of each other are combined to form clusters, single isolated preclusters are also regarded as clusters; 3) clusters with an energy of at least 2 GeV and with at least two particles are called jets if at least $(1-\epsilon)$ of the visible energy E_{vis} is contained in such clusters. The number of jets found in an event yields the jet multiplicity and the sum of the momenta of the particles within a jet gives the jet momentum \vec{k} . The second algorithm, rather than using the angle between two particle momenta \vec{p}_i and \vec{p}_j employs the normalized pair mass $y_{ij} = (p_i + p_j)^2 / E_{vis}^2$, where charged particles are assumed to be pions and neutrals to be photons. If $y_{k,\ell}$ is the lowest value of all possible y_{ij} particles k and ℓ are replaced by a pseudoparticle of four momentum $(|\vec{p}_k| + |\vec{p}_\ell|, \vec{p}_k + \vec{p}_\ell)$. This procedure is repeated until $y_{k,\ell}$ exceeds a given threshold value y_{th}^{max} . The number of remaining pseudoparticles defines the jet multiplicity and their 3-vectors give the jet directions.

The distributions of jet multiplicities obtained by these cluster algorithms depend on the jet defining parameters (ϵ, χ) and y_{th}^{max} . For small y_{th}^{max} and small ϵ as well as small χ many jets are found because of the fluctuations of the hadronisation process, whereas for large y_{th}^{max} and large values of ϵ and of χ mostly 2-jet events are found and the $q\bar{q}g$ -events are not resolved. However, Monte Carlo studies show that there is a range of cluster parameters, for which QCD effects can be resolved and the fragmentation effects are sufficiently small. In the following, the parameters $y_{th}^{max} = 0.04$ and $\epsilon = 0.1$, $\chi = 45^\circ$ are used, which were found to be a reasonable set. With these parameters less than 4% of the events have more than 3 jets, and, using the y -method (ϵ, χ -method), about 30% (20%) have 3 jets and about 70% (80%) have 2 jets.

The analysis is mainly concerned with the class of 3-jet events, for which normalized jet energies $x_i (x_1 > x_2 > x_3)$ are calculated in the following way: the measured jet momenta $\vec{k}_i (|\vec{k}_1| > |\vec{k}_2| > |\vec{k}_3|)$ are projected onto the reaction plane defined to be normal to $(\vec{k}_1 \times \vec{k}_2) + (\vec{k}_2 \times \vec{k}_3)$ and the angle θ_{ij} between these projections determines the normalized jet energies x_i

$$x_i = \frac{2 \cdot \sin^2 \theta_{k\ell}}{\sin^2 \theta_{12} + \sin^2 \theta_{23} + \sin^2 \theta_{31}} ; \quad i, k, \ell \text{ cyclic}$$

which will be compared with the theoretical jet energies x_i of ref. 6) defined by twice the energy going into the i th jet divided by the total energy going into all three jets. There are two independent variables, since $\sum x_i = 2$. We shall analyse the distributions of x_1 , the maximum normalized jet energy, and of $x_1 = x_2 \cdot \sin \theta_{12} = x_3 \cdot \sin \theta_{31}$.

Before confronting the data with corresponding theoretical predictions several corrections have to be applied. The corrections have to account not only for the experimental resolution and the acceptance of the detector and the effects of initial state photon bremsstrahlung, but also for the fluctuations in the hadronisation process, which might for instance cause a primary $q\bar{q}$ -process to be classified as a 3-jet event. We used model calculations to unfold these effects from the raw distributions such that one can compare the corrected distributions with the theoretical predictions directly. The model calculations are based on first order QCD, using a quark gluon

coupling strength $\alpha_S^{(1)} = 0.17$ at $\sqrt{s} = 34$ GeV. They reproduce the measured particle distributions rather well. For details see ref. 10). For the present analysis two different fragmentation schemes were applied, in order to estimate the uncertainties due to hadronisation. In the Lund scheme¹¹⁾, the fragmentation proceeds along the colour flux lines; in the scheme of Ali et al¹²⁾ along the parton directions. As we have shown in ref. 10), these two fragmentation schemes yield significantly different distributions for low momentum particles. The events were generated by Monte Carlo techniques, taking the resolution and acceptance function of the detector into account, and underwent the identical chain of analysis programs and cluster algorithms as the real data. The distribution of jet multiplicities obtained from these two fragmentation models are substantially different only for narrow jet definitions ($y^{\max} \leq 0.02$) and are in reasonable agreement with the observed jet multiplicities for broader definitions ($y^{\max} \approx 0.04$). These model calculations are used to account for the detection probability of a $q\bar{q}$ -event as well as for the background of 3-jet events produced by primary $q\bar{q}$ -processes by relating the number of generated events $N^{q\bar{q}}$ to the number N_n of n -jet events ($n = 2, 3, 4, \dots$) obtained by the cluster algorithms. For instance for the x_1 -distribution:

$$N^{q\bar{q}}(x_1) = a_2(x_1) N_2 + \sum_{x_1} a_3(x_1, \bar{x}_1) N_3(\bar{x}_1) + a_4(x_1) N_4 \quad (1)$$

where x_1 is the generated and \bar{x}_1 the "observed" value of the maximum normalized jet energy. The corrections are applied to the data assuming that the corrected and the observed number of real events are related by the coefficients a_i obtained from the model calculations. The overall corrections can be estimated from Fig. 1), where the raw and the corrected x_1 and x_L distributions are shown. The overall corrections are smaller for the mass method. This fact, however, is not only due to its better efficiency of finding $q\bar{q}$ -events but also to its larger $q\bar{q}$ background. For the jet parameters chosen the corrections are, within the errors, independent of the fragmentation scheme used.

One can now directly compare the corrected distributions of Fig. 1 to the theoretical predictions, which in 1st order, independent of the jet parameters used, are given by²⁾

$$\frac{1}{\sigma} \frac{d\sigma}{dx_1 dx_2} = \frac{2}{3} \frac{\alpha_S^{(1)}}{\pi} \frac{x_1^2 + x_2^2}{(1-x_1)(1-x_2)} \quad (2)$$

where $\alpha_S^{(1)}$ is the quark gluon coupling strength of QCD (in 1st order). Fitting this expression, after integration, to the experimental x_1 and x_L -distribution one obtains the values of $\alpha_S^{(1)}$ listed in table 1. The fit was restricted to $x_1 \leq 0.85$ ($x_L \geq 0.30$), a range, which is sufficiently far away from the artificial separation between $q\bar{q}$ and $q\bar{q}g$ events used in the models to avoid the divergencies in the 3-jet cross section. Both distributions, as well as both jet measures, yield, within the errors, the same first order coupling strength $\alpha_S^{(1)}$; on average $\alpha_S^{(1)} = 0.20 \pm (0.015 \text{ stat.}) \pm 0.03$ (system.). It has been verified, that the resulting value of α_S is essentially unchanged if $\alpha_S = 0.20$ is used as input for the model calculations (a change of the input α_S by a factor of two results in a change of the corrected data by about 20% at $x_1 < 0.85$). The systematic error represents an estimate of the uncertainties due to the jet definition and the different fragmentation schemes and fragmentation parameters used for the corrections. The theoretical expression provides in all cases a good description of the data; in the worst case we obtained a $\chi^2_{DF} = 6.8/5$.

The result is in good agreement with our previous result $\alpha_S^{(1)} = 0.18 \pm (0.03 \text{ stat.}) \pm (0.03 \text{ system.})$ ¹³⁾, which was based on a direct comparison of data and Monte Carlo calculations. For a summary of the results from other experiments see ref. 14). The PLUTO³⁾ and CELLO³⁾ groups, using a similar cluster technique, quote somewhat lower values: $\alpha_S^{(1)} = 0.15 \pm 0.03 \pm 0.02$ at $\sqrt{s} = 30$ GeV and $\alpha_S^{(1)} = 0.16 \pm 0.02 \pm 0.03$ at $\sqrt{s} = 34$ GeV, respectively. One should note, however, that these groups include data up to $x_1 = 0.95$ in the fit, whereas the present analysis is limited to $x_1 \leq 0.85$ for the reasons mentioned above. The inclusion of data up to $x_1 = 0.95$ for instance would in our case result in an average reduction in $\alpha_S^{(1)}$ of about 10% and would yield a somewhat worse fit.

The inclusion of 2nd order terms makes the comparison more complicated, since the theoretical predictions depend on the jet definition. The relevant 3-jet cross section formulae are given in ref. 6 for parton jets defined a) by $(1-\epsilon)$ of the total energy going into 3 cones of full opening angle \hat{c} and b) by an invariant mass cut y . Comparing data and theory, we identify ϵ and y with ϵ and y^{\max} of the corresponding cluster algorithms and take $\hat{c} = 60^\circ$, which, as the model calculations show, corresponds roughly to $\chi = 45^\circ$. In using the formulae of ref. 6, which are derived for massless quarks, we take for the number of flavours $N_f = 3$ since the contribution of heavy quarks to the inner loops is strongly damped. (All primary photon quark couplings are of course properly taken into account by the normalization to σ_{tot} .) Increasing N_f from 3 to 5 changes the QCD predictions by less than 3%. The coupling strengths $\alpha_s^{(1+2)}$ obtained by fitting the theoretical expressions to the data are listed in table 1. As an example, the corresponding best fit curves to the x_1 - and x_2 -distributions are shown in Fig. 2 for the jet definition via invariant mass y . The broken curves in Fig. 2a) show the first order contribution to this fit, which are hardly distinguishable in shape from the full curves. The inclusion of second order terms yields essentially a reduction of the coupling strength of about 20%: on average $\alpha_s^{(1+2)} = 0.165 \pm 0.015$ (stat.) ± 0.03 (system.), where α_s is defined in the $\overline{\text{MS}}$ scheme.

The Abelian vector theory¹⁵⁾ yields first order results identical to QCD (after renormalisation of the quark-gluon coupling strength $\alpha_A = 4/3 \alpha_s$). The second order contributions, however, are much larger, as shown in Fig. 2b) where the (1st + 2nd) order predictions of the Abelian theory* are compared to the data. The theoretical curves are obtained with α_A defined in the $\overline{\text{MS}}$ scheme in analogy to QCD. The larger number of quarks caused by the colour degree of freedom in QCD is simulated by tripling the number of flavours. In this framework the Abelian theory gives in 2nd order reasonable results for the total cross section, $R = R_0 \left(1 + \frac{3}{4} \frac{\alpha_A}{\pi} - 1.65 \left(\frac{\alpha_A}{\pi}\right)^2\right)$. But the differential 3-jet cross section is nearly an order of magnitude below the first order results. This is evident from Fig. 2b), where the full curve is the 2nd order prediction closest to the data. Both a smaller and a larger coupling strength α_A yield a smaller 3-jet cross section, since the order α_A^2 contribution is large and negative.

*) The (1st + 2nd) order 3-jet cross sections for the Abelian vector theory can be read off from the formulae of ref. 6 by simply putting $C_F = 1$, $N_C = 0$ and $N_f = 6 \cdot N_{\text{QCD}}$.

In summary, the observed 3-jet cross sections are in good agreement with the QCD predictions. The inclusion of 2nd-order effects causes a reduction of the QCD coupling strength of about 20% with respect to the 1st-order value $\alpha_s^{(1)}$ yielding $\alpha_s^{(1+2)} = 0.16 \pm 0.015$ (stat.) ± 0.03 (system.). In contrast to this the Abelian vector theory, which in 1st-order is identical to QCD, fails to describe the data in (1st + 2nd)-order.

We are indebted to the PETRA machine group and to the computer group for their excellent support during the experiment and to all engineers and technicians of the collaborating institutions who have participated in the maintenance of the apparatus. We would like to thank O. Nachtmann for useful discussions. This experiment was supported by the Bundesministerium für Forschung und Technologie, by the Education Ministry of Japan and by the UK Science and Engineering Research Council through the Rutherford Appleton Laboratory. The visiting groups at DESY wish to thank the DESY directorate for their hospitality.

jet definition via	fit to distribution	1st_order	(1 st + 2 nd)-order
invariant mass	x_1	0.208 ± 0.015	0.163 ± 0.010
	x_{\perp}	0.205 ± 0.013	0.158 ± 0.010
energy flow	x_1	0.196 ± 0.013	0.170 ± 0.010
	x_{\perp}	0.195 ± 0.013	0.175 ± 0.012

Table 1

Coupling strength α_s resulting from fits of 1st and 1st + 2nd order QCD expressions to the experimental x_1 and x_{\perp} -distributions in the region $x_1 \leq 0.85$ and $x_{\perp} \geq 0.30$. The errors quoted result from the fitting procedure and include no systematic effects.

References

- 1) TASSO-Collaboration, R. Brandelik et al., Phys. Lett. 86B (1979) 243, MARK J-Collaboration, D.P. Barber et al., Phys. Rev.Lett. 43 (1979) 830, PLUTO-Collaboration, Ch. Berger et al., Phys. Lett. 86B (1979) 418, JADE-Collaboration, W. Bartel et al., Phys. Lett. 91B (1980) 142.
For recent reviews see R. Marshall, EPS Conference on HEP, Lisbon, Portugal (1981), (to be published) and Rutherford Appleton Laboratory report RL-81-087,
W. Braunschweig, Proceedings of the 1981 Int. Symp. on Lepton and Photon Interactions at High Energy, Bonn, Germany (1981) p. 68.
- 2) J. Ellis, M.K. Gaillard and G.G. Ross, Nucl. Phys. B111 (1976) 253, T. De Grand, Y. Ng, H.-S. Tye, Phys. Rev. D16 (1977) 3251, G. Kramer, G. Schierholz and J. Willrodt, Phys. Lett. 79B (1978) 249 and erratum 80B (1979) 433.
- 3) TASSO-Collaboration, R. Brandelik et al., Phys. Lett. 94B (1980) 437, PLUTO-Collaboration, Ch. Berger et al., Phys. Lett. 97B (1980) 459, CELLO-Collaboration, H.J. Behrend et al., Phys. Lett. 110B (1982) 329.
- 4) JADE-Collaboration, W. Bartel et al., Phys. Lett. 115B (1982) 338.
- 5) A. Ali, J.G. Körner, G. Kramer, Z. Kunszt, E. Pietarinen, G. Schierholz, and J. Willrodt, Phys. Lett. 82B (1979) 285, and Nucl. Phys. B167 (1980) 454,
K.J.F. Gaemers and J.A.M. Vermaseren, Z. Physik C7 (1980) 81,
T. Chandramohan and L. Clavelli, Phys. Lett. 94B (1980) 409, and Nucl. Phys. B184 (1981) 365,
J.G. Körner, G. Schierholz, and J. Willrodt, Nucl. Phys. B185 (1981) 365.
- 6) K. Fabricius, G. Kramer, G. Schierholz, I. Schmitt, Z. Physik C11 (1982) 315; for a discussion of the mass method see G. Kramer DESY 82-029 (1982).
- 7) T. Gottschalk, Phys. Lett. 109B (1982) 331, showed that the results of Fabricius et al. are consistent with those of R.K. Ellis, D.A. Ross, A.E. Terrano, Phys. Lett. 45 (1980) 1226 in the limit where the two different definitions of "thrust" are identical. See also G. Kramer, ref. 6.

- 8) JADE-Collaboration, W. Bartel et al., Phys. Lett. 88B (1979) 171.
- 9) H.J. Daum, H. Meyer, J. Bürger, Z. Phys. C8 (1981) 167.
- 10) JADE-Collaboration, W. Bartel et al., Phys. Lett. 101B (1981) 129.
- 11) B. Andersson, G. Gustafson, T. Sjöstrand, Phys. Lett. 94B (1980) 211 and earlier references quoted therein; for details see T. Sjöstrand LUTP 80-3, April 1980 and Errata to LUTP 80-3.
- 12) A. Ali, E. Pietarinen, J. Willrodt, DESY-T-80/01.
- 13) JADE-Collaboration, W. Bartel et al., Phys. Lett. 91B (1980) 142, JADE-Collaboration, S. Yamada: Proceedings of the xxth International Conference on High Energy Physics, Madison, WI, 1980.
- 14) W. Braunschweig in Proceedings of the 1981 Int. Symp. on Lepton and Photon Interactions at High Energies, Bonn, 1981 page 68.
- 15) M. Glück and E. Reya, Phys. Rev. D16 (1977) 3242; For a recent comparison with deep inelastic lepton scattering data see H. Abramowicz et al., Z. Phys. C13 (1982) 199.

Figure Captions:

Fig. 1 Raw and corrected x_{\perp} and x_{\perp} -distributions for the two different jet definitions.

Fig. 2 a) The corrected x_{\perp} and x_{\perp} -distributions for the mass method ($y^{\max} = 0.04$) together with the second order QCD best fit. The first order contribution of this fit is indicated by the broken curve. The fit did not include data above $x_{\perp} = 0.85$ for the x_{\perp} -fit and below $x_{\perp} = 0.30$ for the x_{\perp} -fit.

b) The corrected x_{\perp} and x_{\perp} -distributions compared to the second order predictions of the Abelian theory, for three different coupling constants α_A . The one yielding results closest to the data corresponds to the full line. The dotted line shows the predictions for a coupling constant smaller than the "best fit" and the broken line for a bigger one. The ϵ , χ jet definitions have been used for these plots.

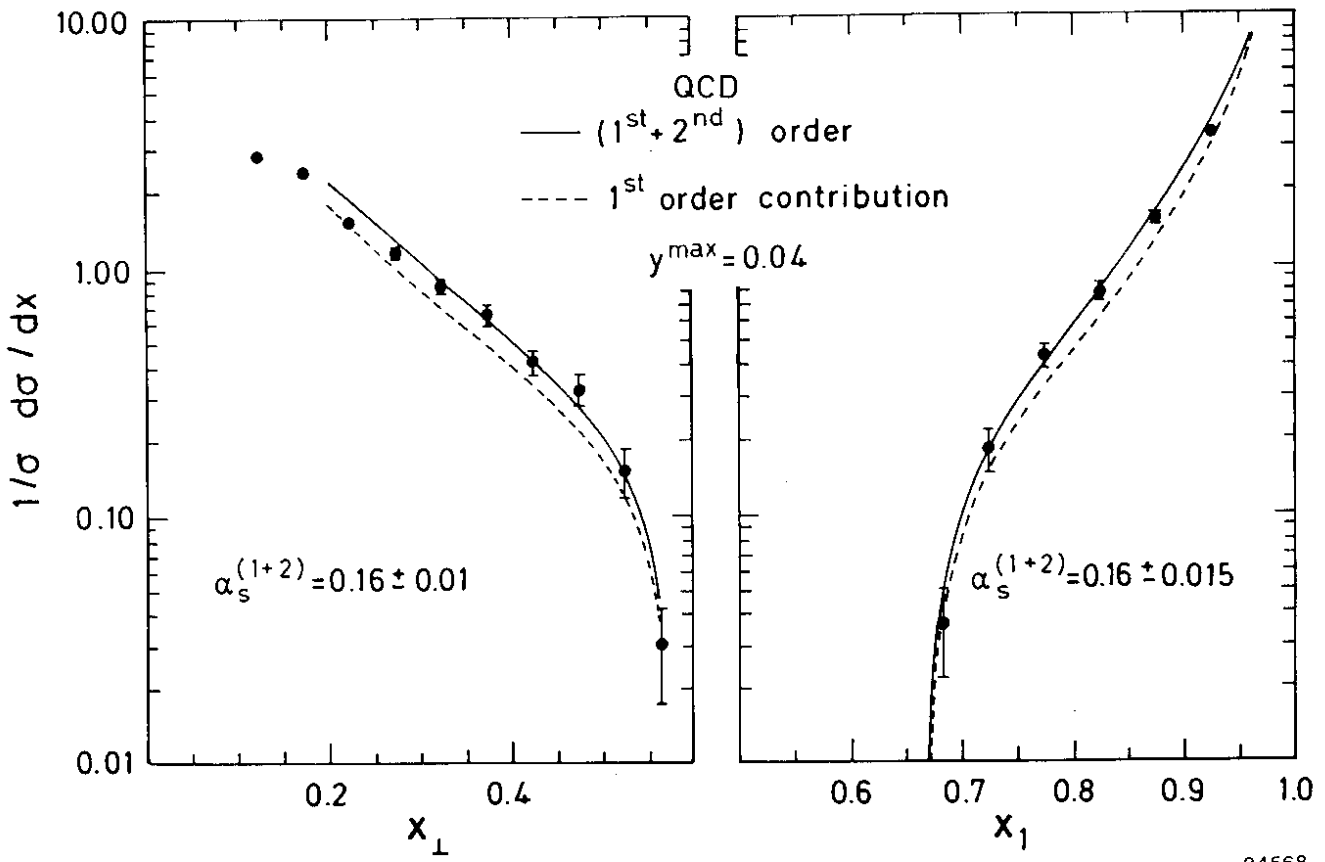


Fig. 2a

34568

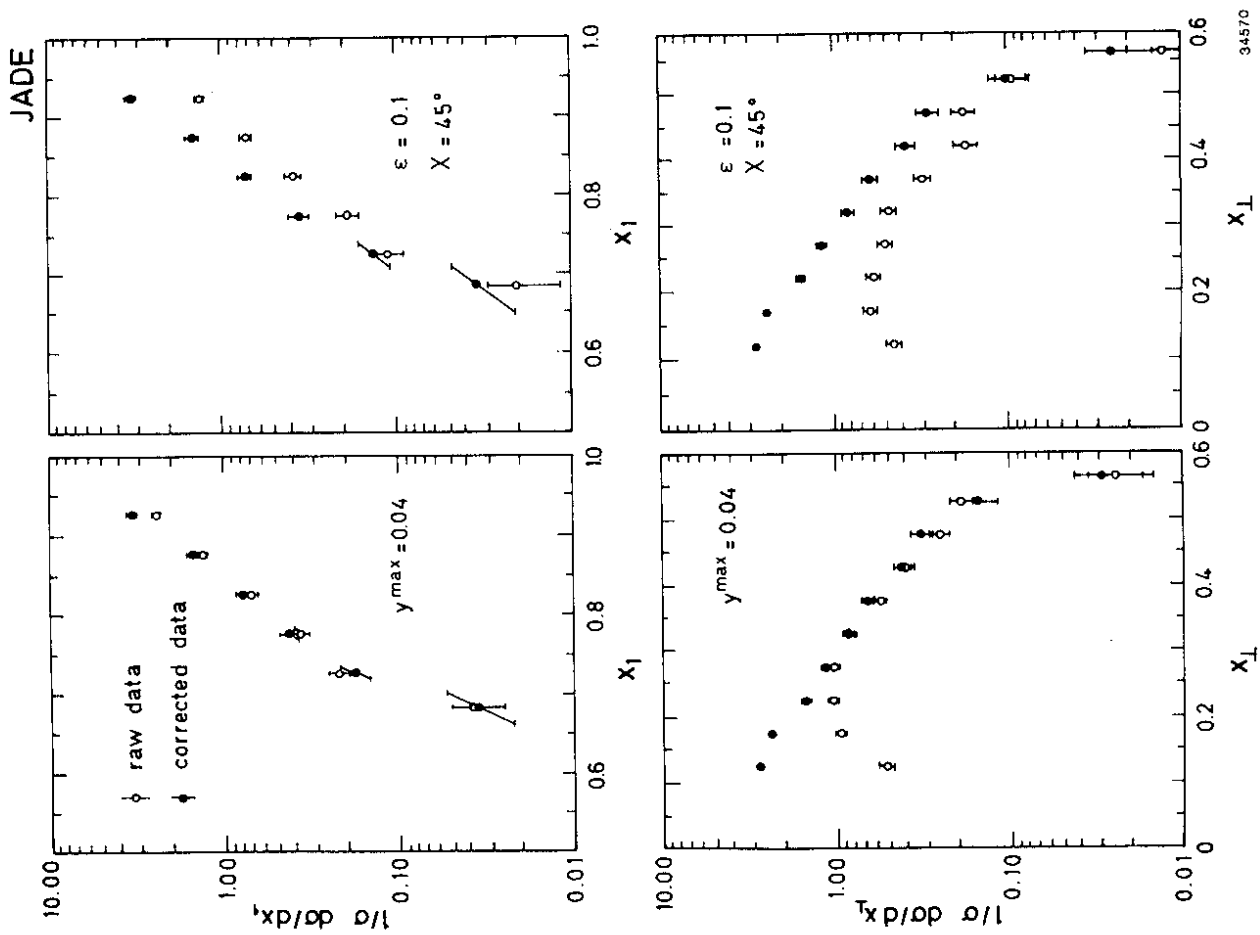


Fig. 1

34570

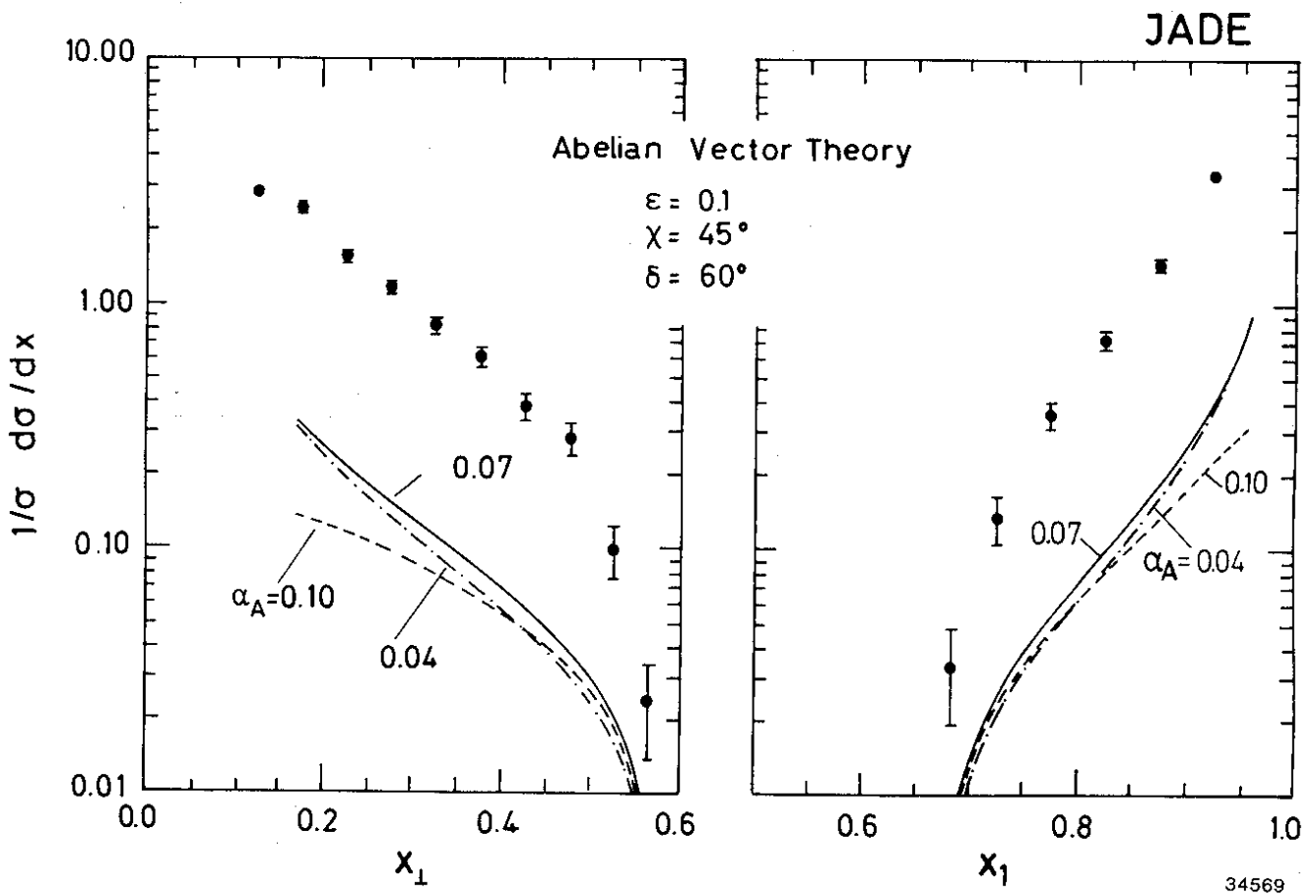


Fig. 2b